05

Ultrathin cerium oxide layers for forming submicron YBCO structures

© E.A. Arkhipova, M.V. Zorina, D.V. Masterov, S.A. Pavlov, A.E. Parafin, P.A. Yunin

Institute for Physics of Microstructures of the Russian Academy of Sciences, Nizhny Novgorod, Russia
E-mail: parafin@ipmras.ru

Received November 17, 2025
Revised November 17, 2025
Accepted December 10, 2025

Nanometer-sized layers of cerium oxide (CeO_2) on sapphire and the characteristics of the YBCO layers deposited on them, depending on the CeO_2 growth temperature, have been studied. It is shown that the use of ultrathin CeO_2 layers obtained at a reduced growth temperature opens up the possibility of forming superconducting epitaxial YBCO structures with submicron element sizes using the preliminary topology mask method.

Keywords: thin films, formation of the topology of the structure, YBCO, cerium oxide.

DOI: 10.61011/TPL.2026.04.63201.20575

Cryogenic electronics based on $Y_1Ba_2Cu_3O_{7-x}$ (YBCO) high-temperature superconductor (HTSC) films has a wide range of applications at present. Josephson junctions were used to construct contact arrays [1], design voltage standards [2], terahertz signal generators [3], detectors [4,5], and low-noise amplifiers and mixers [6,7]. Owing to their low surface resistance, HTSC films are used in high-frequency devices [8]. Current limiters based on HTSC films also find application in high-current electronics [9].

The methods of examination and fabrication of structures based on YBCO films have reached maturity [10]. The topology of a superconducting circuit is set by etching or ion implantation of a functional superconductor film. Owing to the high sensitivity of YBCO films to external influences, the associated technological operations exert a negative influence on the resulting parameters of formed structures and devices.

We have already proposed an alternative method for forming planar superconducting structures on cubic zirconia [3] and sapphire [11]: preliminary topology mask (PTM). The topology is set in it by pre-growth local modification of the substrate (before the YBCO deposition), and the circuit pattern is formed in the course of YBCO deposition onto the modified substrate. The following YBCO growth features are used in this case:

— a high-quality superconducting epitaxial film forms in the standard YBCO growth regime on *r*-cut sapphire (Al_2O_3) with a sublayer of epitaxial cerium oxide (epiCeO_2) [12,13];

— a YBCO layer deposited in the same growth regime onto a specially modified substrate is non-superconducting and forms the separation regions of a superconducting circuit.

The substrate is modified in the following way. A mask defining the circuit pattern is formed from amorphous cerium oxide (coldCeO_2) deposited by laser sputtering without heating the substrate. Cerium oxide is then deposited onto the substrate in the epitaxial growth regime (hotCeO_2). An epiCeO_2/Al_2O_3 forms on sapphire in the mask windows. Outside of these windows, the coldCeO_2 layer prevents epitaxy, and a non-epitaxial hotCeO_2/coldCeO_2/Al_2O_3 region is formed on it. With subsequent magnetron deposition of YBCO, it grows non-epitaxially in the hotCeO_2/coldCeO_2/Al_2O_3 regions, forming a separating insulating region, while an epitaxial YBCO film grows on the surface of epitaxial cerium oxide (i.e., in the epiCeO_2/Al_2O_3 regions), forming a superconducting region. Since amorphous cerium oxide is deposited without heating the substrate, simple lift-off lithography (with an optical resist for micrometer sizes or an electronic resist for submicrometer sizes) is used to form the pattern. It is important that there are no formal restrictions on thickness of a YBCO functional film deposited on a substrate with an already specified topology. The advantage of the PTM method is that post-growth processing of a „thick" YBCO film is excluded from the technological process, and circuit elements are shaped in accordance with the pattern of amorphous cerium oxide.

The formation of YBCO structures with minimal dimensions by PTM requires simultaneous fulfillment of the following conditions: low roughness of the epiCeO_2 layer; minimum thickness of epiCeO_2 at which high performance characteristics of the YBCO film are retained; minimum thickness of the coldCeO_2 layer at which a separating non-superconducting YBCO/hotCeO_2/coldCeO_2/Al_2O_3 region is formed. Three series of structures were fabricated for this purpose.

In the first series, the properties of YBCO/epiCeO_2/Al_2O_3 structures, which were used for comparison with ultrathin layers, were examined as functions of the deposition temperature of a 50-nm-thick epiCeO_2 layer. The YBCO deposition conditions remained unchanged; the film thickness was 70 nm. The results are presented in Fig. 1: surface roughness R_a of epiCeO_2 (arithmetic average roughness height within a scan $2 \times 2\,\mu$m in size measured by atomic force microscopy); half-width of the rocking curve of reflection $\Delta\omega(002)$ of epiCeO_2, which characterizes the

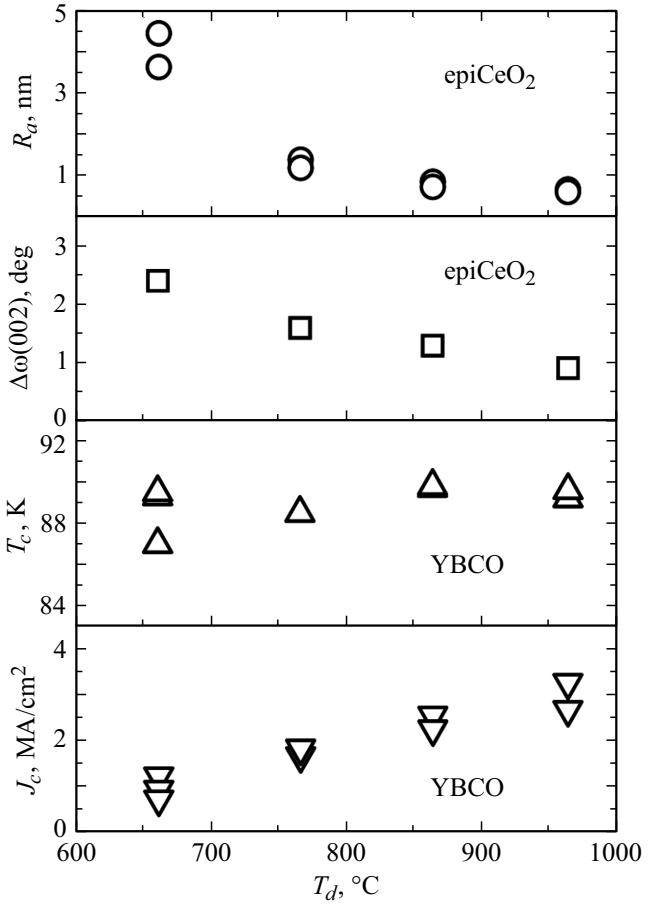

Figure 1. Roughness R_a of epiCeO$_2$, misorientation $\Delta\omega(002)$ of epiCeO$_2$ mosaic blocks for 50-nm-thick layers, and characteristics (T_c and J_c) of YBCO films grown on these layers as functions of growth temperature of the epiCeO$_2$ layer.

misorientation of mosaic blocks of the cerium oxide layer; and critical temperature T_c and critical current density J_c (at 77 K) of the YBCO film. The $\Delta\omega(005)$ values of YBCO were below 1°.

The second series of structures differed only in the thickness of epiCeO$_2$. An ultrathin (3 nm) epiCeO$_2$ layer was chosen based on the results reported in [14], where the possibility of growth of high-quality YBCO films on such a layer was demonstrated. The results are presented in Fig. 2: roughness R_a of epiCeO$_2$ and T_c and J_c (77 K) of the YBCO film. Measurements of $\Delta\omega(002)$ of ultrathin epiCeO$_2$ layers were not performed, since the signal from such layers was very weak. The values of $\Delta\omega(005)$ of YBCO for this series were also below 1°.

The surface roughness and the misorientation of mosaic blocks of the 50-nm-thick epiCeO$_2$ layer decrease significantly with an increase in growth temperature T_d. The minimum values are found at $T_d = 960$ °C: $_2$ $R_a = 0.7-0.8$ nm and $\Delta\omega(002) = 0.9°$, which is indicative of fine crystalline quality of the epiCeO$_2$ layer that may be achieved only through epitaxial growth. The T_c value of YBCO films varies only slightly with the growth temperature of epiCeO$_2$. The maximum value of $J_c = 3$ MA/cm^2 was obtained at growth temperature 960 °C, which is the highest one examined.

The surface roughness of a 3-nm-thick epiCeO$_2$ layer is, in contrast to that of a „thick“ (50 nm) layer, remains low within the entire range of growth temperatures. The value of R_a for epiCeO$_2$ in this case is 0.05–0.08 nm, which is comparable to roughness $R_a = 0.05$ nm of the original sapphire substrate. The epitaxial growth of cerium oxide layers is confirmed indirectly by the fact that YBCO epitaxial films grown on them have fine superconducting characteristics. It is interesting that, in contrast to the „thick“ epiCeO$_2$ layer, critical current density J_c of YBCO films on ultrathin layers reaches its maximum (exceeds 3 MA/cm^2) at low deposition temperatures (660–760 °C) and decreases only slightly with increasing epiCeO$_2$ deposition temperature.

To estimate the resistance of the insulating region, we fabricated the third series of structures: YBCO/epiCeO$_2$/Al$_2$O$_3$ regions separated by a YBCO/hotCeO$_2$/coldCeO$_2$/Al$_2$O$_3$ gap 10 μm in width. The thickness of amorphous coldCeO$_2$ layers was chosen within the range from 3 to 24 nm corresponding to the thickness limit for lift-off lithography with an electron resist. As in the second series, the epiCeO$_2$ thickness was 3 nm. Following YBCO deposition, the resistance of the separation region was measured at $T = 77$ K. The obtained resistance values had a significant spread and increased as the time of storage of structures increased. Therefore, the results in the table are sorted for clarity into three groups: with resistances less or greater than 3 kΩ/sq and with superconducting leakage. The value of 3 kΩ/sq is much higher than the resistance of

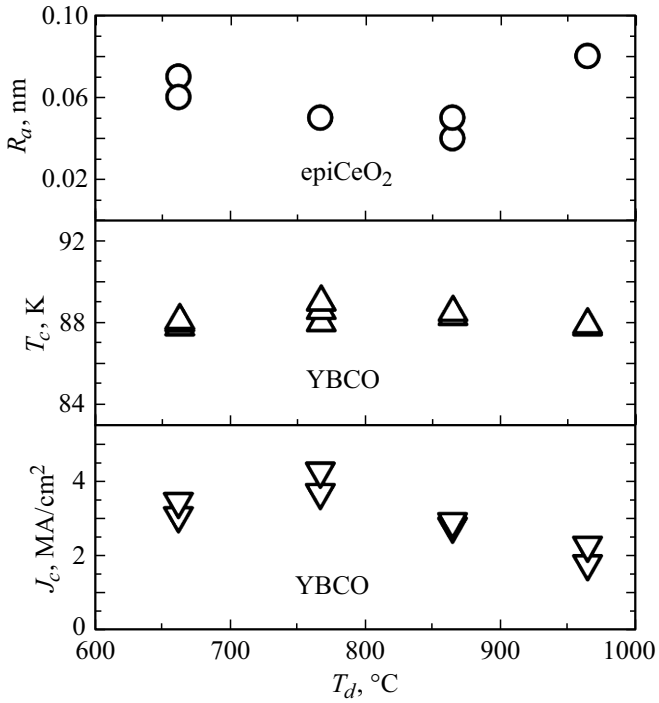

Figure 2. Roughness R_a of epiCeO$_2$ for 3-nm-thick layers and characteristics (T_c and J_c) of YBCO films grown on these layers as functions of growth temperature of the epiCeO$_2$ layer.

Characteristics of the separation region of the structure with coldCeO_2 layers of various thickness t (0 — superconducting region, dash (−) — resistance lower than 3 kΩ/sq, N — resistance higher than 3 kΩ/sq, and T_d — epiCeO_2 growth temperature)

t, nm	T_d, °C			
	660	760	860	960
3	0	0	–	0
6	*N*	0, –	–	0
12	*N*	*N*	*N*	0, –
24	*N*	*N*	*N*	–

the YBCO film in the normal state; i.e., it is sufficient to form a separating region. The data presented in the table demonstrate that a coldCeO_2 layer 6 nm in thickness is sufficient to form a high-resistance separation region at a growth temperature of epiCeO_2 660 °C. When T_d of epiCeO_2 increases, the characteristics of the insulating region deteriorate.

Thus, it was demonstrated that the characteristics of YBCO/epiCeO_2/Al_2O_3 within the range of growth temperatures of epiCeO_2 660−960 °C behave differently depending on the thickness of epiCeO_2:

— the optimum temperature for an epiCeO_2 sublayer 50 nm in thickness is 960 °C;

— an ultrathin (3 nm) epiCeO_2 sublayer has a lower roughness, and the optimum characteristics of the YBCO film are achieved at a lower temperature of 660−760 °C.

It was found that the growth of the ultrathin (3 nm) epiCeO_2 sublayer in the YBCO/epiCeO_2/Al_2O_3 structure at a reduced temperature of 660 °C allows one to both maintain the high performance characteristics of the YBCO superconducting film and reduce the thickness of amorphous cerium oxide in the insulating region of YBCO/hotCeO_2/coldCeO_2/Al_2O_3 down to 6 nm.

Thus, such small thicknesses of cerium oxide layers provide an opportunity to form YBCO structures with submicrometer-sized superconducting elements and insulating regions by the preliminary topology mask method.

Acknowledgments

Equipment provided by the Center for Collective Use „Physics and Technology of Micro- and Nanostructures“ (Institute for Physics of Microstructures, Russian Academy of Sciences) was used in the study.

Funding

This study was supported by the Russian Science Foundation, grant No 24-29-00824, https://rscf.ru/project/24-29-00824/.

Conflict of interest

The authors declare that they have no conflict of interest.

References

[1] R. Kandari, S. Kumar, N. Khare, Appl. Phys. A, **131**, 545 (2025). DOI: 10.1007/s00339-025-08666-w
[2] A.M. Klushin, J. Lesueur, M. Kampik, F. Raso, A. Sosso, S.K. Khorshev, N. Bergeal, F. Couëdo, C. Feuillet-Palma, P. Durandetto, M. Grzenik, K. Kubiczek, K. Musiol, A. Skorkowski, IEEE Instrum. Meas. Mag., **23** (2), 4 (2020). DOI: 10.1109/MIM.2020.9062678
[3] L.S. Revin, D.A. Pimanov, A.V. Chiginev, A.V. Blagodatkin, V.O. Zbrozhek, A.V. Samartsev, A.N. Orlova, D.V. Masterov, A.E. Parafin, V.Yu. Safonova, A.V. Gordeeva, A.L. Pankratov, L.S. Kuzmin, A.S. Sidorenko, S. Masi, P. de Bernardis, Beilstein J. Nanotechnol., **15**, 26 (2024). DOI: 10.3762/bjnano.15.3
[4] E.I. Glushkov, A.V. Chiginev, L.S. Kuzmin, L.S. Revin, Beilstein J. Nanotechnol., **13**, 325 (2022). DOI: 10.3762/bjnano.13.27
[5] O. Volkov, V. Pavlovskiy, I. Gundareva, R. Khabibullin, Y. Divin, IEEE Trans. Terahertz Sci. Technol., **11** (3), 330 (2021). DOI: 10.1109/TTHZ.2020.3034815
[6] T. Zhang, J. Du, Y.J. Guo, IEEE J. Microwaves, **2** (3), 374 (2022). DOI: 10.1109/JMW.2022.3171675
[7] M. Malnou, C. Feuillet-Palma, C. Ulysse, G. Faini, P. Febvre, M. Sirena, L. Olanier, J. Lesueur, N. Bergeal, J. Appl. Phys., **116**, 074505 (2014). DOI: 10.48550/arXiv.1405.5998v1
[8] S. Ariyoshi, H. Mikami, A. Ebata, S. Ohnishi, T. Hizawa, S. Tanaka, K Nakajima, Mater. Res. Express, **8**, 116001 (2021). DOI: 10.1088/2053-1591/ac3693
[9] L. Liang, Y. Wang, P. Pang, Z. Yan, Z. Deng, J. Magn. Magn. Mater., **604**, 172283 (2024). DOI: 10.1016/j.jmmm.2024.172283
[10] Yu. Divin, Appl. Sci., **13** (9), 5766 (2023). DOI: 10.3390/app13095766
[11] D.V. Masterov, S.A. Pavlov, A.E. Parafin, P.A. Yunin, Tech. Phys. Lett., **42** (6), 594 (2016). DOI: 10.1134/S1063785016060110.
[12] S. Bevilacqua, S. Cherednichenco, IEEE Trans. Terahertz Sci. Technol., **4** (6), 653 (2014). DOI: 10.1134/S0021364007230075
[13] M. Tarasov, E. Stepantsov, A. Kalabukhov, M. Kupriyanov, D. Winkler, JETP Lett., **86** (11), 718 (2008). DOI: 10.1134/S0021364007230075.
[14] A.V. Boryakov, D.V. Masterov, S.A. Pavlov, A.E. Parafin, P.A. Yunin, Phys. Solid State, **66** (6), 818 (2024). DOI: 10.61011/PSS.2024.06.58691.20HH.

Translated by D.Safin